Impact of COVID-19 on spatio-temporal variation of aerosols and air pollutants concentration over India derived from MODIS, OMI and AIRS

Yashwant B. Katpatal[1] · Vikas K. Patel[2] · Digambar S. Londhe[1]

Abstract

The atmospheric aerosols and air pollutants affect the earth's atmosphere, human health and climate system. Human-induced aerosols and air pollutants are the major causes of the deterioration of air quality. The COVID-19 lockdown restricted the movement of people and vehicles, stopped industrial and agricultural activities and may have impacts on the aerosols in the atmosphere. Spatio-temporal map of MODIS Terra AOD_550 nm, OMI Aura UVAI, Ozone, NO_2, SO_2 and AIRS CO during the lockdown illustrates the significant reduction in their concentration. During the lockdown, the North India shows a record reduction of over 20% in Aerosol Optical Depth and Aerosol Index values. A substantial decrease in AOD and AI was also observed in Eastern and Western parts of India. The average AOD value were reduced from 1.36 (2016–2019) to 1.09 (2020) over India during the lockdown. The satellite-retrieved aerosol variables over India recorded lowest AOD values on 29th March, 2020 (0.2566) and 21st April 2020 (0.2591). Similarly, air pollutants CO, NO2 and SO2 also significantly reduced in India. Despite all variables showing a reduction in concentration, Ozone recorded an increase in value during lockdown primarily over North and North-eastern parts of India. Western India recorded a substantial reduction in SO_2 (47%) followed by Central India (31%). As pan India is considered, CO was reduced by 1%, NO_2 reduced by 15.29% and SO_2 was reduced by 26.82% during the lockdown period. This abrupt reduction in aerosol and air pollutants concentration over India was mainly due to the lockdown of COVID-19.

Keywords Aerosol · COVID-19 · Ozone · Aerosol optical depth · Aerosol index

1 Introduction

India is facing air pollution, climate change problem from decades. Air pollution has emerged as a significant environmental issue due to rise in population, surge in vehicular traffic emission and growing industrialization and urbanization as it harms human health and significant economic losses [1]. Undoubtedly, the atmosphere is certainly more polluted in the last few decades, especially in developing countries. According to World Health Organization [2], global air pollution caused nearly 7 million deaths (nearly

11.6% of the deaths) in 2012 making it the greatest single environmental health risk in the world. Out of 640 districts in India, 27% in 1998 exceeded the yearly standard value of 40 g/m^3 and 45% in 2010 [3]. Kumar et al. (2023) [4] have presented scientometric analysis and evaluation by using 26,859 documents retrieved from available database on exposure to air pollution and health. Nine cities out of the top 10 most polluted cities in the world by the World Health Organization are from India [5]. Thus, this situation is a complicated issue, which strongly influences human health and a demanding solution is required in order to maintain the air quality level. The primary pollutants (examples are CO, CO_2, NO_2 and SO_2) are the pollutants that are released directly into the atmosphere, usually from domestic, industrial, or transportation sources, while secondary pollutants are gases and particulates that also form in the atmosphere, largely from the primary pollutants. The chemical composition of air pollutants, such as their oxidising power, solubility, concentration and the susceptibility of the affected

✉ Yashwant B. Katpatal
ybkatpatal@rediffmail.com

1 Department of Civil Engineering, Visvesvaraya National Institute of Technology, Nagpur, Maharashtra 440010, India

2 CORAL, Indian Institute of Technology Kharagpur, Kharagpur 721302, India

person or object, largely determines the level of damage they can do. Due to their water solubility, SO_2 gases can harm human skin and bronchi. In contrast, O_3 and NO_2 gases can enter the lungs more deeply due to their lower solubility [6].

The contribution of aerosols in causing climate change and air pollution cannot be ignored. Aerosols also have a significant contribution to the energy balance of the earth-atmospheric system. Thus, studies focusing on aerosol properties and their distribution are required for generating a better understanding of the phenomena of regional and global climate change [7]. The ambient air quality is highly determined by aerosols. Aerosols, also known as particulate matter, are known to be a major contributor to air pollution, particularly in developing nations like China and India which is also affecting human health [8, 9].

The tropospheric aerosols have a large spatial and temporal variability as they have irregular distribution, widespread origin and short residence time in the atmosphere and anthropogenic events like festivals affect the aerosol patterns [10]. Aerosols are generated by anthropogenic and natural sources directly into the atmosphere and are also produced by various physical and chemical processes in the atmosphere [11]. The distribution of atmospheric aerosols and their impact on the earth's climate system is not understood completely and remains a concern to both the scientific community and policymakers [12]. Aerosols cause scattering and absorption of solar radiation and thus influence climate directly [13–15], while it influences climate indirectly by affecting the processes like cloud condensation droplet concentration, cloud optical properties, precipitation rates and a lifetime of clouds [16].

Aerosol Optical Depth (AOD) and Aerosol Index (AI) are quantitative estimates of the aerosols present in the atmosphere and are generally used as a substitute for particulate matter in the atmosphere. AOD is an optical parameter and an indicator of the extinction effect of atmospheric aerosols which is used to determine the degree of air pollution. AI is a qualitative index indicating the presence of higher-concentration layers of aerosols with significant absorption in the atmosphere. Several studies have been carried out to develop a relationship between empirical satellite-derived AOD and particulate matter [17]. AOD is a measure of the quantum of energy absorbed or reflected by airborne particles as it is transmitted through the atmosphere. AI monitoring has been used worldwide to find out air pollution sources, analyse dispersion and migration patterns of air pollutants across continents, measure air quality and its prediction and also study the energy balance between radiations and factors of climate change [18]. The magnitude of AI is controlled by the optical depth of aerosols, the type of aerosol i.e., the composition and origin and the altitude of the aerosol layer and the view angle [19]. The smoke and desert dust particles which are absorbing aerosols show

positive values of AI while scattering aerosols are given negative values [20]. However, the values of AI may also be negative due to other factors like high altitude clouds and variations in surface reflectance [21]. AI values near zero indicates the presence of clouds [22], while AI values greater than 1.0 indicate the presence of absorbing aerosols like soot or dust particles [23].

The world was facing the Coronavirus disease (COVID-19) which is a pandemic caused by severe acute respiratory syndrome coronavirus 2 (SARS-CoV-2). Worldwide millions of people have been affected by COVID-19 and many of them lost their life. The disease was first detected in December 2019. On 30th January 2020, the Government of India (GOI) confirmed India's first COVID-19 case. As the number of confirmed COVID-19-positive cases was increasing, to break the chain or to reduce the spread of this pandemic, on 24th March 2020 the GOI imposed a nationwide lockdown 1.0 for 21 days from 25th March to 5th April. The lockdown was further extended by 19 days from 16th April to 3rd May which was termed lockdown 2.0. The lockdown virtually restricted 1.3 billion people of India from stepping out of their homes, all transport services such as road, rail and airways were suspended except transportation of essential goods and services. Educational institutions, industrial establishments, construction and agricultural activities were also suspended.

Second aspect of this problem is to validate the fact that the anthropogenic activities are contributing significantly in causing the air pollution. This can only be verified if the anthropogenic activities are either stopped or slowed down and then the air pollution status is monitored. As air quality has deteriorated in most of Indian cities over the past few decades, this lockdown provided an excellent opportunity [24–26] to study how the atmosphere responds to a rapid and abrupt reduction in pollution produced by various anthropogenic activities, such as industries, biomass burning, transportation, etc. This was also an opportunity to distinguish between the possible impacts of natural and anthropogenic aerosols and air pollution in the atmosphere. Hence, the present study was conducted using the satellite data products to analyse the anticipated changes in the air pollution status in India during the lockdown period which presented an opportunity of reduced anthropogenic activities and compare this scenario with scenario of increased anthropogenic activities in the previous years. This study aims to analyse the aerosols loading along with the concentration of gaseous air pollutants over pan India during the lockdown in India using Moderate Resolution Imagin Spectroradiometer (MODIS) Terra, Ozone Monitoring Instrument (OMI) Aura and Atmospheric Infrared Sounder (AIRS) Aqua satellites. The previous related studies also analysed the air pollution scenarios for lockdown period [27] in which they compared PM2.5 and NO_2 concentration. They utilized data

from continuous Ambient Air Quality Monitoring Stations (CAAQMS) of Central and State Pollution Control Boards in India for 2018, 2019 and 2020 over six Indian cities. The study also investigates the spatio-temporal variation and time series analysis of aerosols and air pollutants over India during the lockdown period and its comparison to previous years. The present study determined the CO, NO_2, SO_2, ozone, AOD and AI using satellite data. However, a detailed location-based analysis can be performed and validated elaborately if more ground observation data is available for number of cities in India.

2 Materials and methods

2.1 Study area

The present study of aerosol loading has been performed over pan India. India has high topographical heterogeneity of aerosol and meteorological properties. The extent of India is bounded by the latitude of 6°44′–35°30′ N and longitude of 68°7′–97°25′ E. The area is marked by large variations in temperature across different seasons. The mean temperatures in the region vary between 10 °C in winter to about 32 °C in summer.

Urbanization, industrial activities, agricultural activities and energy utilization are rapidly expanding, resulting in increased anthropogenic emissions and air quality deterioration. In the present study, to analyse the impact of COVID-19 on aerosol loading and air pollution, India has been divided into six regions namely North India (NI), South India (SI), West India (WI), East India (EI), Central India (CI) and North-East India (NEI) as shown in Fig. 1. The green line in Fig. 1 represents the line of Himalayan Mountain Range which acts as the obstruction to the movement of air in the atmosphere.

WI, EI and SI are bounded by long stretch coastal region where sea salt aerosols may play an important role while NI part is bounded with the great Himalayan Mountain range, which acts as a barrier, trapping the aerosols and air pollutants over the region. In NI, the Indo-Gangetic plain (IGP) (Fig. 1) is regarded as one of the most polluted areas, where anthropogenic activities, especially agricultural burning, are mostly to blame for greater aerosol loading [28]. The IGP has the highest population density in India and is characterized by large sources of emission from precursors of aerosols and air pollutants. WI comprises the desert area as well as the long-stretch coastal region where desert dust aerosol may play an important role. This desert dust is transported by wind also to the atmosphere of NI primarily during the summer season which contributes to higher aerosol concentration in the region. Due to the increase in population, urbanization

has increased which has resulted in an increase in the consumption of fossil fuel while biomass burning in the rural areas has led to high aerosol loading over India.

2.2 Data used

Satellites can provide a unique opportunity to monitor and evaluate air quality in order to fill gaps in ground-based measurements, thereby improving our understanding of aerosol contributions to energy balances, air pollution and climate change. Integration of satellite-based continuous monitoring of aerosols and pollutants and measurements using in-situ surface techniques is probably the best proposition to understand the impacts of aerosols on climate and human health. Three Earth Observation System (EOS) satellites MODIS Terra, Aqua and OMI Aura have made daily global aerosol observations over the past two decades. Because of its wide availability, the present study uses the MODIS Terra satellite products for AOD, OMI Aura for AI, Ozone, NO_2, SO_2 and AIRS Aqua for CO as given in Table 1.

The instruments assess the AOD measurements from reflected solar radiation, radiative transfer measurements and using aerosol models based on spectral responses. A proper collection of AOD satellite data over the region under consideration is necessary to correctly estimate the amount of aerosols over that region [29]. The AI is the difference between measured and estimated spectral contrast of two near UV wavelengths [30]. This spectral contrast is in fact due to differences in the response of absorbing aerosols and also because of phenomena like reflection, scattering, absorption and dispersion from the surface, gases, clouds and aerosols respectively [20]. This range is useful for aerosol detection over land as in the ultraviolet wavelengths; the land has low surface albedo [31]. The OMI Aura is the first satellite which is working on UV and visible spectrum with the charge-coupled device, enabling daily, global monitoring of Ozone, NO_2 and SO_2 [32, 33].

To carry out this study, satellite data of AOD, AI, CO, NO_2, Ozone and SO_2 for the period 25 th March to 3rd May 2016–2020 has been obtained from the Giovanni portal of Goddard Earth Science Data and Information Services Centre, NASA. Satellite instruments that measure NO_2 are sensitive to the number of molecules between the instrument and the Earth's surface (i.e., a Vertical Column Density or VCD). For NO_2 typically the amount high in the atmosphere (in the stratosphere) is removed in order to provide an estimate of the column in the lower part of the atmosphere (the troposphere), a Tropospheric Vertical Column Density or TVCD. The units of VCD or TVCD are molecules per square centimeter or mol/cm^2. The description of data products obtained from different satellites is given in Table 2.
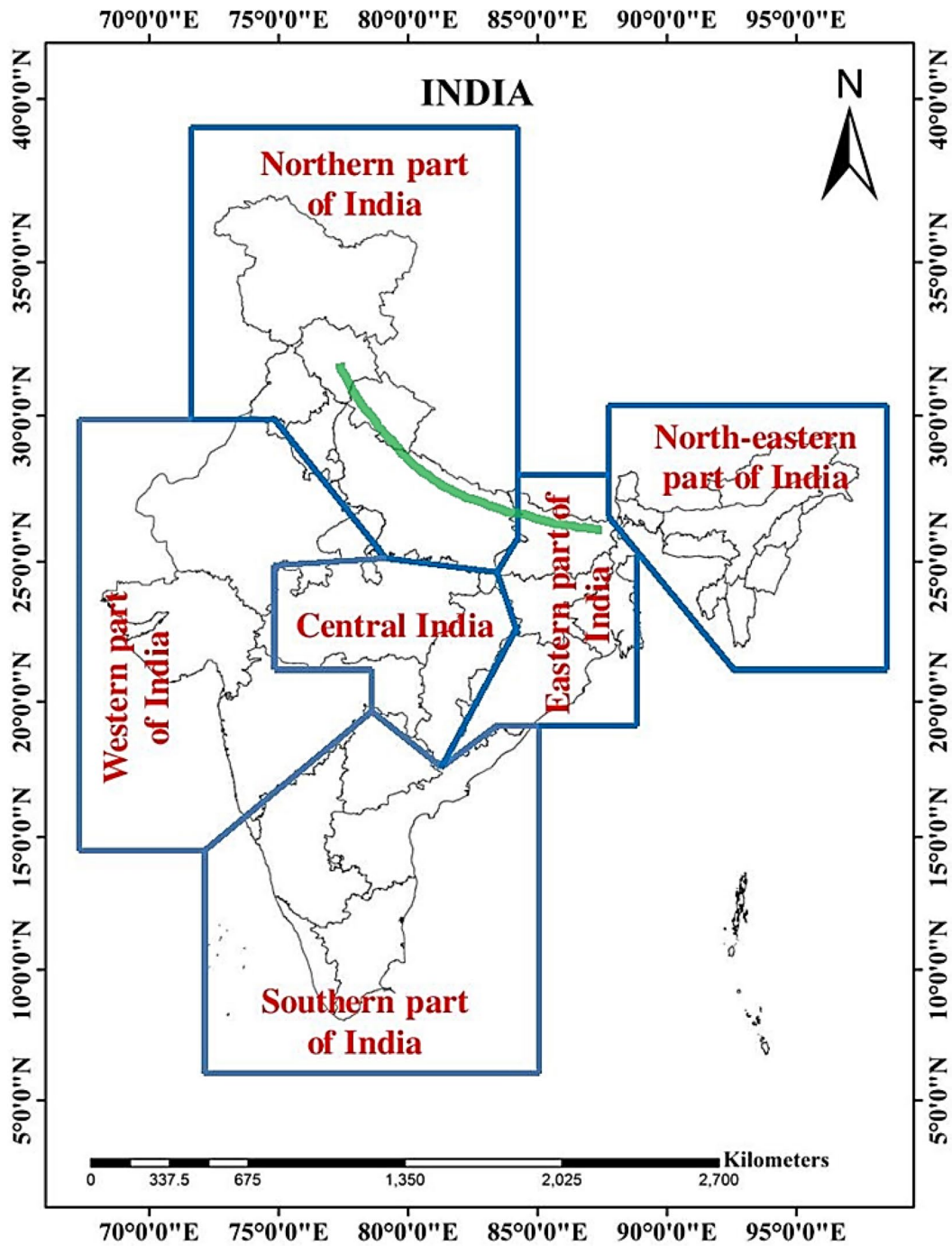
Fig. 1 Geographical location of India including 6 regions selected for study

Table 1 Description of satellite/sensor used in this study

Satellites/sensors	EOS mission	Year of launch	Spatial resolution	Temporal resolution	Wavelength range
MODIS	Terra and Aqua	1999 and 2002	250 m, 500 m and 1000 m	1 to 2 days	0.4 um to 14.4 um
OMI	Aura	2004	13 km * 24 km	1 days	0.27 um to 0.5 um
AIRS	Aqua	2002	13.5 km * 13.5 km	1 to 2 days	3.7 um to 15.7 um

Table 2 Properties of satellite data products of aerosols and air pollutants obtained from Giovanni

Satellite/Sensor	Parameter	Grid	Temporal resolution	Wavelength	Product level	Unit	Remark
MODIS-Terra	AOD	1°	Daily	550 nm	MOD08_D3_v6.1	Unitless	Dark Target algorithm
OMI-Aura	AI	1°		UV	OMTO3_v003	Unitless	–
	Ozone	0.25°		UV	OMDOAO3_v003	DU	*DAOS
	SO$_2$	0.25°		310–340 nm	OMSO2e_v003	DU	*BARD
	NO$_2$	0.25°		405–465 nm	OMNO2d_v003	mol/cm^2	30% cloud screened
AIRS	CO	1°		4.6 um	AIRS3STD_v006	ppbv	*DA @850 hpa

*DAOS (Differential Optical Absorption Spectroscopy): Algorithm use to derive total ozone column from OMI Aura satellite [34]

*BRD (Band Residual Difference Algorithm): Used for retrieval of SO$_2$ data in planetary boundary layer from OMI Aura [35]

*DA (Daytime/Ascending): In this study DA of CO used at 850 hpa where ascending means equatorial crossing South to North @1:30 PM

2.3 Methodology

The overall methodology adopted to perform the analysis involves spatial analysis of the satellite data described above to determine AOD, AI, gaseous air pollutant concentrations in the atmosphere for pan India. These parameters were determined for the lockdown period (25th March to 3rd May 2020) and were compared with similar parameters determined for 2016–2019 scenarios. The steps involved in the methodology are as below.

1. The above satellite retrieval daily data of aerosol and gaseous pollutants for the period of 25th March to 3rd May 2016–2020 has been averaged over India and also for the selected six regions using raster calculator tools in the ArcGIS environment.
2. To study the impact of the lockdown during COVID-19 on different regions of India, spatio-temporal maps of AOD, AI and air pollutants over India as well as bar charts have been plotted for each region during the lockdown period of 2020 and 2016–2019.
3. The percentage change analysis of air pollutants between the year 2020 and the average of 2016–2019 from 25th March to 3rd May has been carried out to observe the impact of the lockdown on these pollutants. During lockdown periods, heavy to light precipitation has been observed over a major part of India. Hence, to analyse the impact of precipitation on aerosol concentration in the atmosphere, a time area average map is generated for AOD, AI and precipitation.
4. In the atmosphere, gaseous air pollutants have the ability to react with each other which may affect the concentration of other pollutants. The atmospheric chemistry of air pollutants also leads to the formation of fine aerosol particles. A spatial correlation study of aerosol variables (AOD and AI) and air pollutants (Ozone, CO, NO$_2$ and SO$_2$) has been performed for the lockdown period using Giovanni tools.

3 Results and discussion

3.1 Spatial variation of AOD and AI over India during lockdown period

The average MODIS Terra AOD at 550 nm from 25th March to 3rd May for the 2016–2019 average and 2020 is represented in Fig. 2. This spatial map illustrates that, during the lockdown period, MODIS Terra recorded lower AOD values (0.15–0.40) over NI. It may clearly be observed in Fig. 2, that AOD values are very high over NI relative to other regions during 2016–2019. The Indo-Gangetic plain in NI is a highly polluted region, where anthropogenic aerosols are dominant, but due to complete lockdown with no human activities, significantly low AOD values (0.33) have been observed primarily over NI and also over other regions of India. The AOD values have been observed over NI (0.33), CI (0.29), WI (0.26), SI (0.34), EI (0.46) and NEI (0.47). Present study shows that significantly lower AOD values have been observed for the first time in last five years. The percentage reduction in last 5 years in overall AOD values across India is 26.67% while reduction was 25% and 29.41% in CI and EI respectively.

NEI showed relatively higher AOD values (0.40–0.70) during lockdown relative to other regions. These higher AOD values during lockdown may be due to the wind direction and velocities which bring aerosol particles from other places to the atmosphere of NEI. SI and WI also show relatively lower AOD values 0.34 and 0.46 respectively. For the last two to three decades, anthropogenic aerosols are a major concern and IPCC has also mentioned in its assessment report the impact of aerosols on Earth's climate system and their uncertainties [36]. The present study also gives a clear picture of how anthropogenic activities are majorly responsible for the deterioration of air quality; IGP in NI is a strong example of this.

Similarly, average AI maps have been generated for the 40 days (25th March to 3rd April) lockdown period for
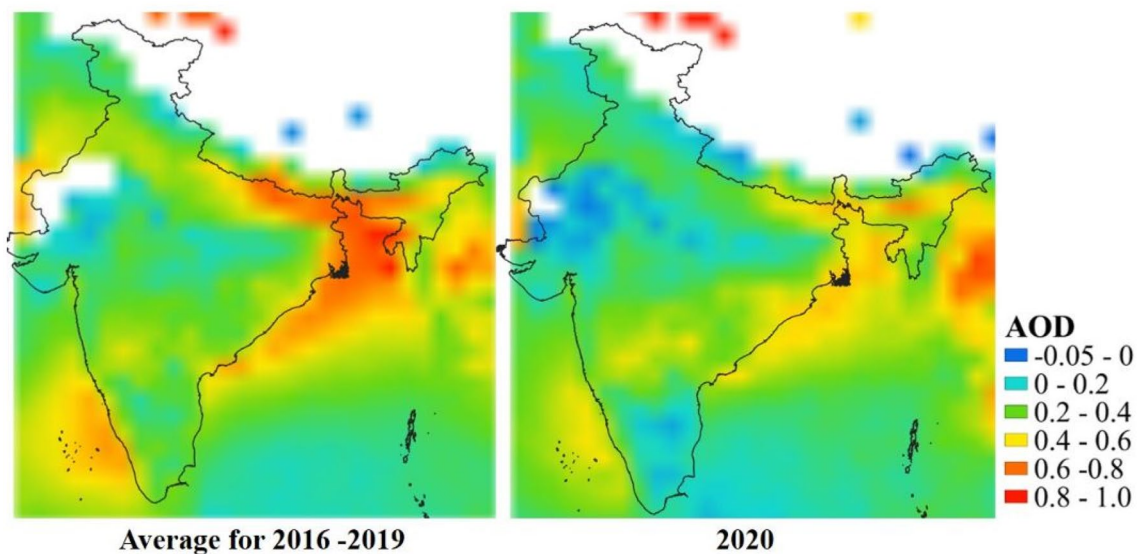
Fig. 2 Variation of MODIS AOD @ 550 over India during 25 March to 3 May 2020 (lockdown period) and average of 2016–2019 for same period

2020 and 2016–2019 as shown in Fig. 3. Since the effect of aerosols and the atmospheric process in UV bands is more intense, the AI is considered as an indication of UV absorbing aerosols like soot and desert sand particles [20]. In all the years, the entire India shows an AI value of greater than zero i.e., no negative value. AI values are observed positive for absorbing aerosols (smoke and dust) and negative for non-absorbing aerosols (sulphate and sea salt). It means that non-absorbing particles are not dominant in India [37].

In the year 2020, results clearly show that entire India shows low AI value (AI < 1) than the average of 2016–2019

where AI values of more than 1 are also observed over some parts of India mainly over NI (IGP). Over NI and NEI, an AI value of greater than 1.5 (Fig. 3) has also been observed in past years. This may be due to the dust aerosol particles over the region transported by wind from the Thar region, or the dust particles originating through wind erosion and the absorbing aerosols like black carbon or organic carbon generated by anthropogenic activities.

During the lockdown period, all possible sources of black carbon and soot emissions such as industrial activities, transportation and biomass burning were suspended in
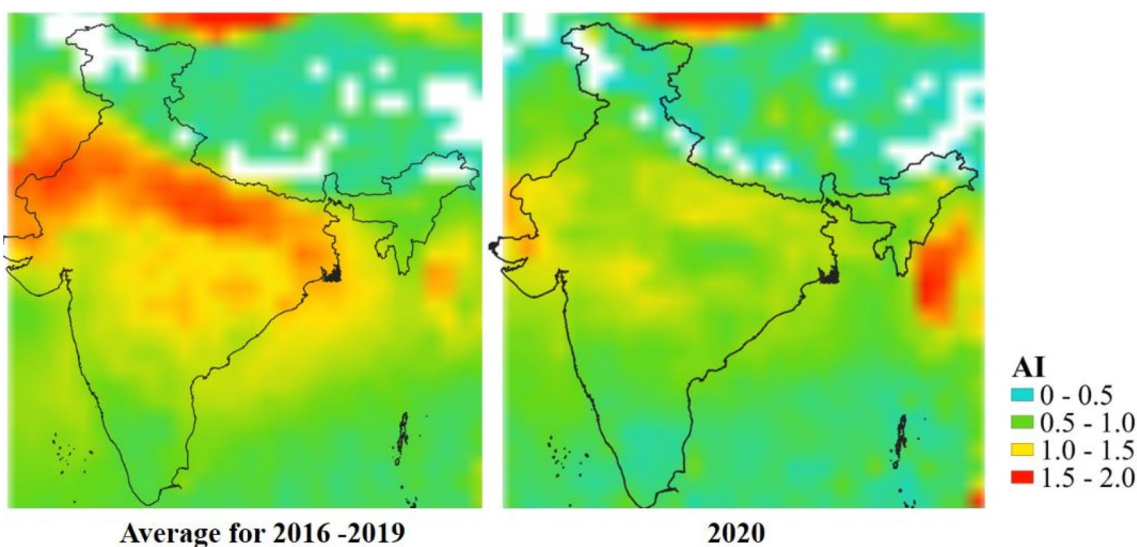

Fig. 3 Variation of OMI Aura UV AI over India during 25 March to 3 May 2020 (lockdown period) and average of 2016–2019 for same period

the country,, hence lower values of AI were recorded compared to previous years. These parameters of aerosol loading clearly show a record low value of aerosol over India during the lockdown period compared to other years which indicates a clear sky without fine or coarse particulate matter primarily over NI and EI.

3.2 Regional variations of AOD and AI during lockdown period

Bar charts histograms have been generated (for AI and AOD) over all six regions of India during the lockdown period of 2020 and the same period during 2016–2019. It is clearly observed that AI is decreased over all the regions except NEI during lockdown period as shown in Fig. 4. It may be due to wind patterns that transport dust, sea salt and other types of aerosols from NI and EI as well as from the neighbouring countries. During the lockdown period, AI values of 1.03(NI), 1.17(CI), 1.26(WI), 1.14(EI)), 0.87(SI) and 1.07(NEI) have been observed compared to 1.42(NI), 1.55(CI), 1.56(WI), 1.58(EI), 1.10(SI) and 0.96(NEI) in

2016–2019 (Fig. 4). Average AI value of 1.09 (2020) has been observed over India relative to 1.36 (2016–2019), which indicates approximately 19.85% reduction. Among all regions, average AI values over NI (1.03) and SI (0.87) are lower than India's average (1.09).

Similarly, all regions show lower AOD values during the lockdown period compared to an average of 2016–2019. It is clearly observed from Fig. 4 that average AOD values over EI (0.44) and NEI (0.48) are higher compared to other regions. Nearly a 21.3% reduction in average AOD value has been observed due to the lockdown compared to values in 2016–2019. The average AOD in India is 0.36(2020) compared to 0.44 in previous years. NI (0.33), CI (0.29), WI (0.26) and SI (0.34) show lower values compared to India's average AOD (0.36) whereas EI (0.46) and NEI (0.47) show higher AOD values. Each region gives a clear picture of how human-induced aerosols play a significant role in polluting the environment. The results of the AOD estimated from MODIS data has been validated with AERONET data for Kanpur City. The results show that the average AOD of Kanpur city for the years 2016–2019 is 0.575 while the average
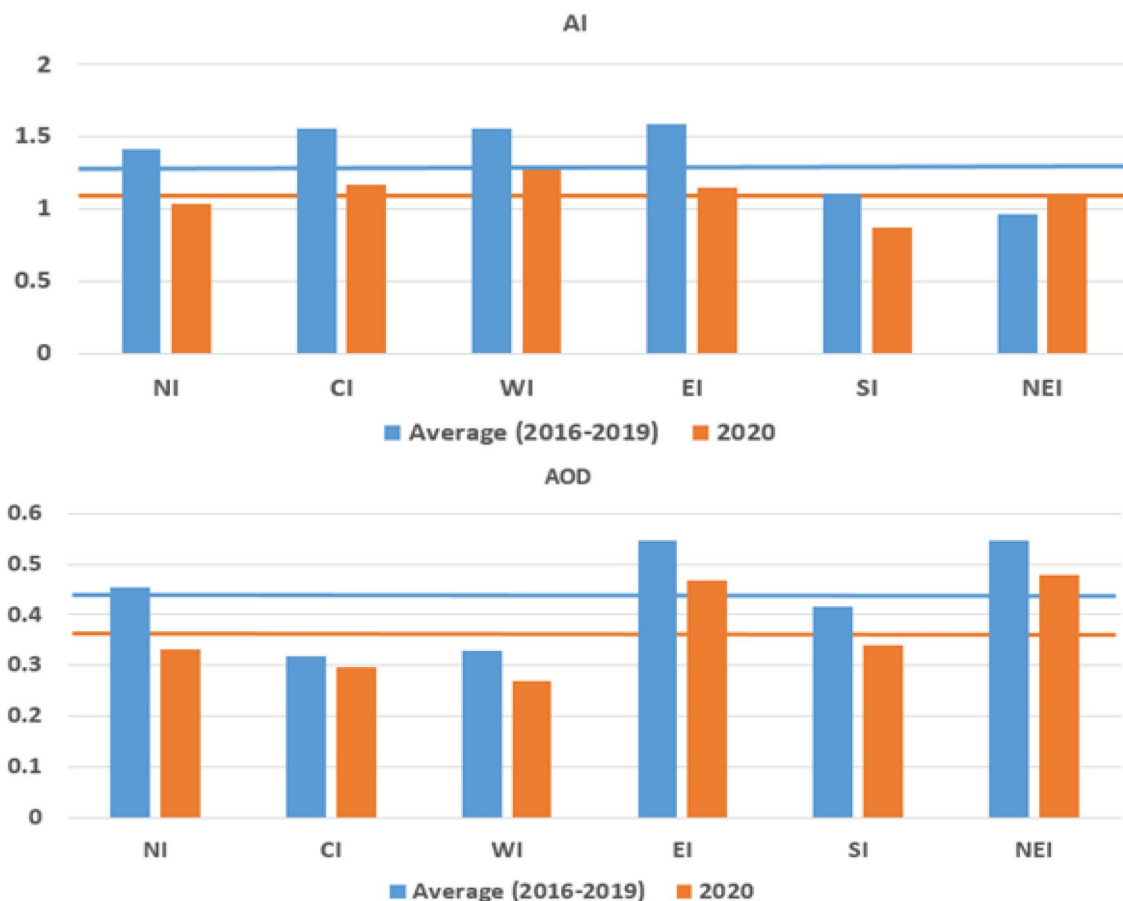

Fig. 4 MODIS AOD @ 550 nm and OMI Aura UV AI variation over NI, CI, WI, EI, SI, NEI during lockdown period and horizontal line indicates India's average for AOD and AI

AOD of Kanpur for April 2020 which was lockdown month was 0.440. This shows that AERONET data is also indicating reduction in AOD value for North India [38].

Histogram displaying frequency and OMI @UV-AI has been generated for the period 25th March to 3rd May for 2020 and 2019 over India (Fig. 5). During the lockdown period, more frequency has been observed for AI range of 0.5–1.5 compared to 0.5–2 in 2019. Nearly zero frequency is observed for AI value beyond 2.5 in 2020 compared to 3.5 in 2019 (Fig. 5). In spite of the maximum value (4.05) of AI observed during the lockdown period, it shows a low mean (1.15) and standard deviation (1.10) compared to 2019 (3.83, 1.34 and 1.28).

3.3 Temporal variation of AOD, AI and precipitation during lockdown period

Average time series plots of AOD, AI and precipitation (precipitation data has been obtained from GPM satellite during the lockdown period at a spatial resolution of 0.1 degree) over pan India has been generated during the lockdown period. Results clearly show that during the first week of lockdown, a sharp drop in AOD values is observed while AI shows relatively low constant values (Fig. 6). This sudden drop in AOD value is due to both lockdown and heavy rains (around 25th March, 18th April and 26th April an average rainfall of 7 mm, 6 mm and 6.5 mm respectively is observed) (Fig. 7) which cleaned the aerosols from the atmosphere. But after rainfall events, it is observed that the AOD value gradually increases (till 18th April) but it never goes beyond 0.5 except on 15th April as shown in Fig. 6.

Gradual increase in AI is also observed over India from 30th March to 18th April. After the 18th of April, both AOD and AI show a drastic decrease in their values till the 21st of April and after that, both parameters gradually increase. The fitted line for AOD during lockdown also illustrates a lower and nearly constant value of 0.35 over India but AI show's slightly increasing pattern.

During the 40 days lockdown period of 2020, AOD was almost zero two times precisely on 29th March and 21st April. In the time period during which AOD and AI values are lower, high precipitation was also observed at some places over India where aerosols were washed out or rain out with rain droplets. After the rainfall events in such areas, there was less increase in aerosol loadings over India which leads to better atmospheric conditions. This lower value of AI over India is mainly due to the lockdown and partially due to rainfall events during the lockdown over some parts of India primarily over NI, EI and SI as shown in Fig. 7.

3.4 Spatio-temporal variation and change analysis of Ozone, CO, NO$_2$ and SO$_2$

Spatio-temporal variation maps of CO, Ozone, NO$_2$ and SO$_2$ has been generated for 25th March to 3rd May 2020 and an average of 2016–2019 to analyse the variation of air pollutants. During the lockdown period, NO2 (Fig. 8a) has significantly decreased over all regions of India such as NI (− 20%), CI (− 16%), WI (− 13%), SI (− 19%), EI (− 18%) and NEI (− 3%) (Table 3). Among all six regions, EI shows a higher concentration of NO$_2$ (5.085×10^{15} mol/cm^2) whereas, over NEI, a lower concentration of 4.26×10^{15} mol/cm^2 has been observed (Table 3).

Similarly, SO$_2$ also shows a significant decrease in values over all regions as mentioned in Table 3. Volcanic SO$_2$ is frequently pumped into the atmosphere above the planetary
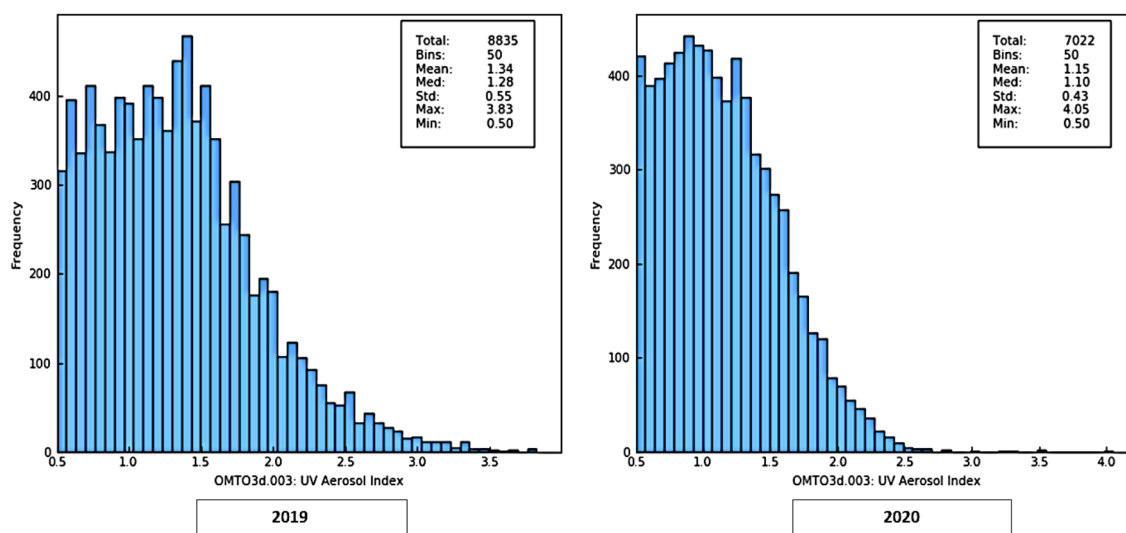

Fig. 5 Histogram map of OMTO3d.003: UV Aerosol Index illustrating frequency of AI value during lockdown period
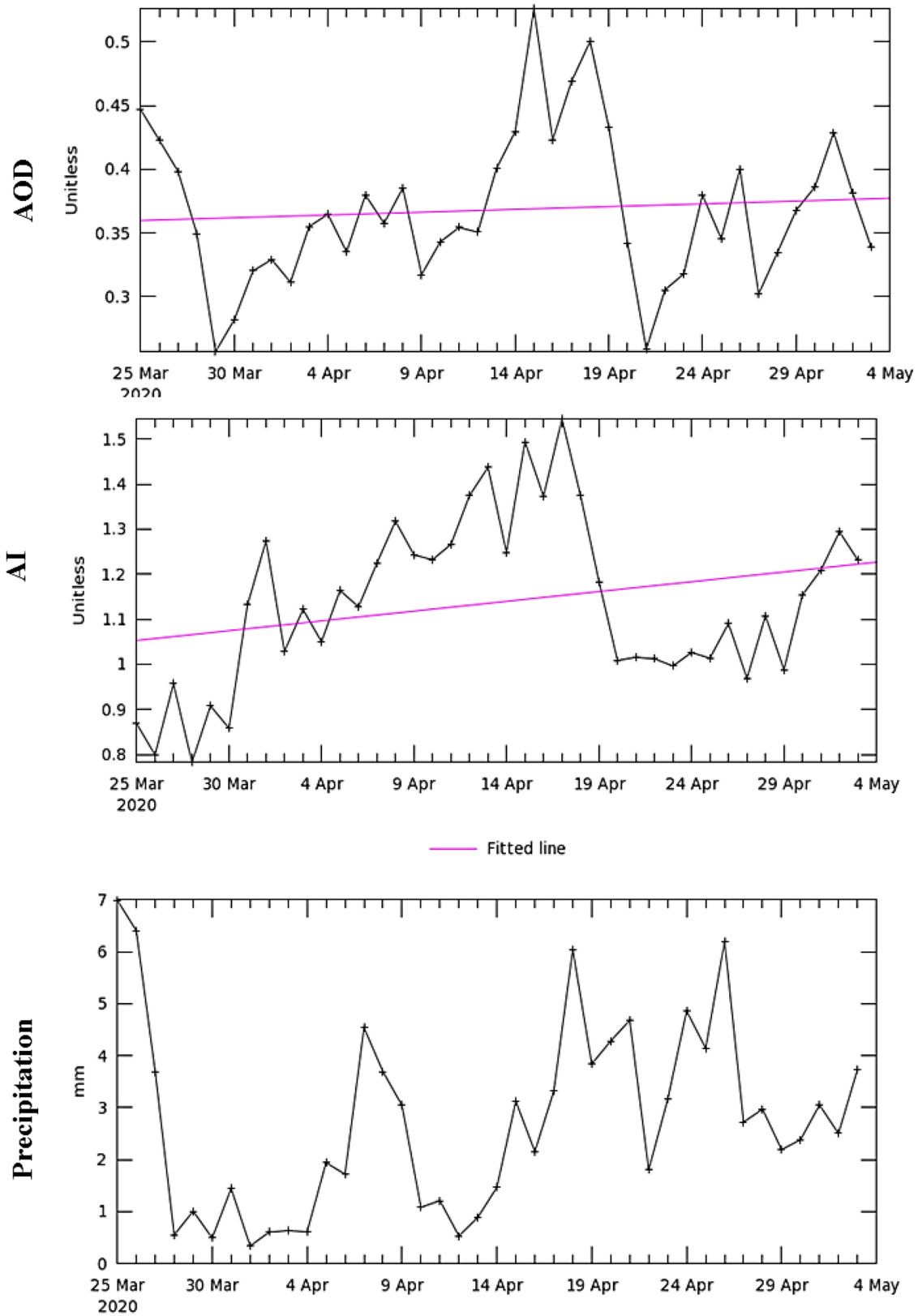
Fig. 6 Time area average map over India of AOD, AI and Precipitation which describe the variation during lockdown period and impact of precipitation on aerosols
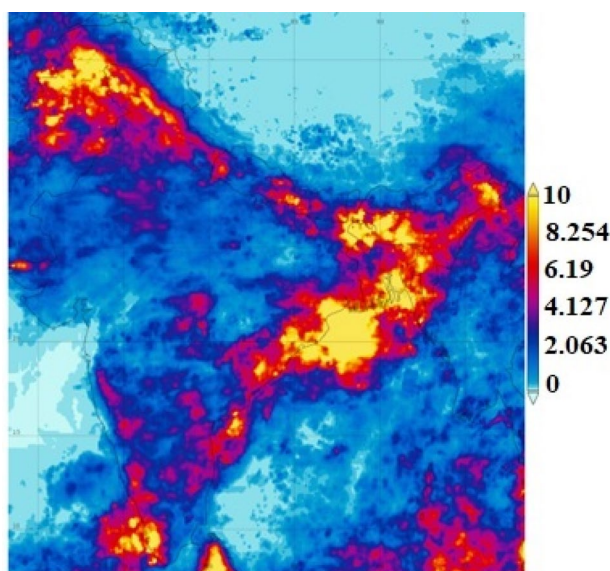
Fig. 7 Time averaged map of daily accumulated precipitation over 25th March to 3rd April 2020

boundary layers at high altitudes, while anthropogenic SO_2 emissions predominate in or just above the planetary boundary layers. From the spatial map of SO_2 which is recorded by OMI in the planetary boundary layer, it may be clearly observed that EI is mostly influenced by SO_2 pollutants and it may be due to high coal-related activities over the region [39]. The highest reduction in SO_2 concentration has been observed during the lockdown period over WI (-47.38%) followed by CI (-31%) and EI (-27.85%) (Table 3).

Compared to previous years, in lockdown period of 2020, Ozone concentration has increased over all the regions primarily over NI (5.07%) and NEI (4.62%) (Table 3). NO_2 plays an important role in the formation of Ozone; NO_2 shows decreasing values over all the regions, but ozone shows increasing values (Fig. 8b and Table 3). This may be another factor that affects the formation of Ozone in the atmosphere [40]. Burning of agricultural residue and biomass generates CO, but this 40-day lockdown has not allowed such activities. Despite lower values, EI and CI show more concentration compared to previous years (Fig. 8b and Table 3). Of all the regions, more reduction in CO concentration has been observed over NI (5.14%). This lower concentration may be due to fewer biomass-burning activities during lockdown as NI is strongly known for such types of activities [41].

3.5 Spatial correlation of aerosols and gaseous air pollutants during lockdown period

3.5.1 Relation between AOD, AI and SO$_2$

AI and AOD are critical variables in the estimation of aerosols in the atmosphere, estimating the intensity of atmospheric pollution and examining their impacts on climate. Both parameters measure aerosol concentration at different wavelengths. In the spatial correlation map between AOD and AI (Fig. 9) over India during the lockdown period, WI and EI show a positive correlation with an average correlation coefficient of 0.60 while NEI and CI show a negative correlation, while average correlation coefficient of 0.63 has been observed over India. This spatial correlation variation of AOD and AI over different regions may be due to atmospheric dynamics, atmospheric chemistry, types of aerosols and wavelength at which satellite sensors recorded these variables.

In India, major sources of SO_2 in the atmosphere are coal power plants where black carbon and soot particles are also released along with SO_2 which is measured in the form of AOD and AI and particulate matter. In both the spatial correlation maps (AOD vs. SO_2 and AI vs. SO_2), it is clearly observed that entire India does not show a positive correlation (Fig. 9). A positive correlation is observed at a particular location where mostly coal power plant is situated or coal activity is observed. SO_2 is also responsible for the generation of fine secondary aerosols through atmospheric chemistry in the atmosphere [42].

3.5.2 Relation between Ozone, NO$_2$ and CO

NO_2 is crucial for the formation of ozone through photochemical oxidation. The spatial correlation map clearly illustrates that the IGP region in NI and SI shows a positive correlation (Fig. 9; NO_2 vs. Ozone). IGP is a highly polluted region in India that is mostly polluted by anthropogenic activities where a higher concentration of NO_2 is due to vehicular emission and biomass burning. Since, NO_2 in the stratosphere play a critical role in ozone layer depletion by itself, it has been observed in the present study that there is an increase in ozone concentration from 2016 to 2019 average concentration when compared to 2020 lockdown period concentration (Fig. 8b). It is also observed that there is a decrease in the NO_2 concentration from 2016 to 2019 average concentration when compared to 2020 lockdown period concentration (Fig. 8a).

The average correlation coefficient of 0.62 has been observed between NO_2 and CO over the IGP region during the lockdown period (Fig. 9; NO_2 vs. CO). CO is mostly released from agricultural residue or biomass burning and vehicular pollution. Strong biomass burning, high industrial

Fig. 8 **a** Spatio temporal variation of OMI SO$_2$ and OMI NO$_2$ over India during lockdown period. **b** Spatio temporal variation of OMI ozone and AIRS CO over India during lockdown period
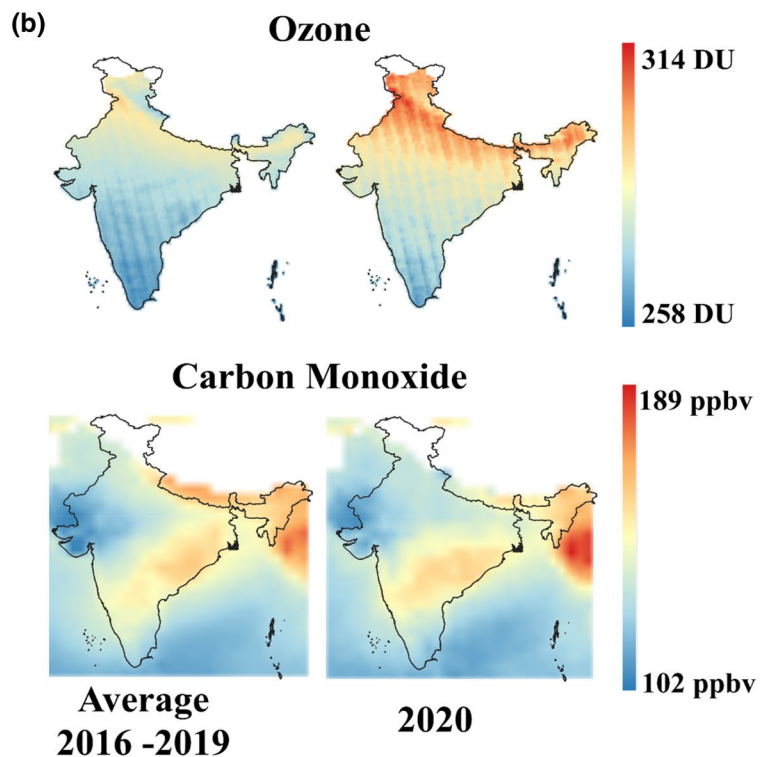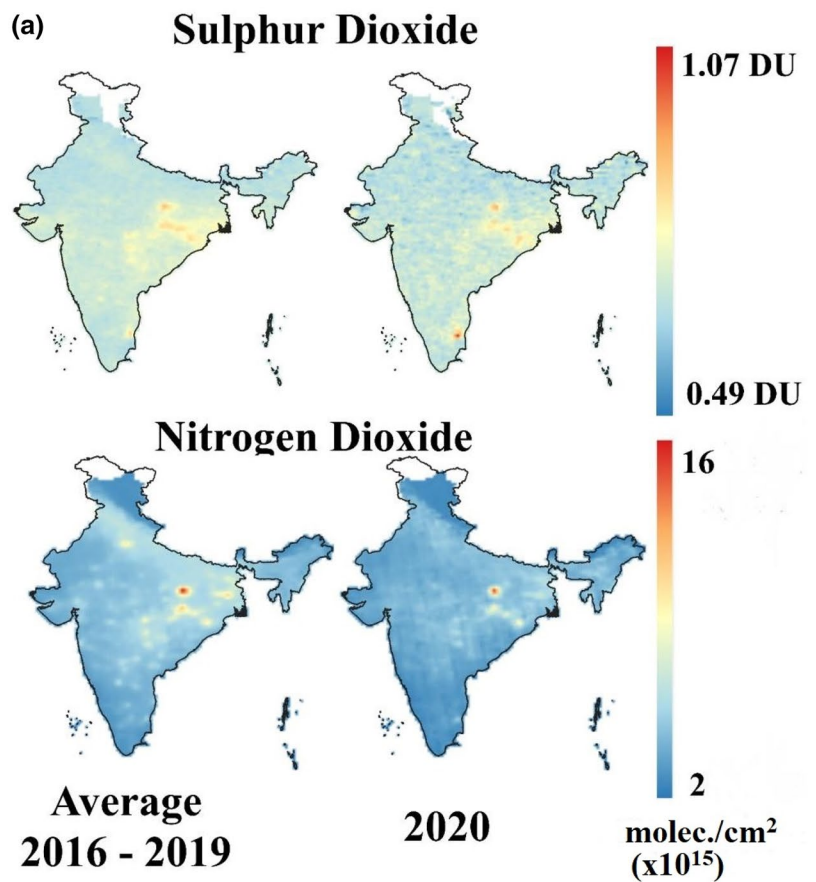
Table 3 Percentage change in the value of CO, Ozone, NO$_2$ and SO$_2$ during lockdown period over different regions of India compare to average of 2016–2019

Region	Parameter	Mean		Standard Deviation		% Change (Mean)
		2016–2019	2020	2016–2019	2020	
NI	CO	133.744	126.867	74.090	3.264	− 5.14
NI	Ozone	284.839	299.282	4.407	4.954	5.07
NI	NO$_2$	5.438E+15	4.341E+15	1.575E+15	1.137E+15	− 20.17
NI*	SO$_2$	1.988E−04	− 1.963E−02	6.428E−02	9.441E−02	–
CI	CO	132.221	135.624	10.746	7.575	2.57
CI	Ozone	275.499	285.315	2.519	3.787	3.56
CI	NO$_2$	5.799E+15	4.857E+15	1.230E+15	9.043E+14	− 16.26
CI	SO$_2$	9.196E−02	6.341E−02	1.026E−01	1.085E−01	− 31.05
WI	CO	120.576	125.062	11.368	11.655	3.72
WI	Ozone	276.100	285.400	4.734	6.551	3.37
WI	NO$_2$	4.800E+15	4.164E+15	7.422E+14	5.073E+14	− 13.26
WI	SO$_2$	4.191E−02	2.205E−02	7.300E−02	8.089E−02	− 47.38
SI	CO	135.318	134.573	8.013	10.670	− 0.55
SI	Ozone	267.809	274.474	2.990	4.475	2.49
SI	NO$_2$	4.440E+15	3.578E+15	8.132E+14	5.967E+14	− 19.41
SI	SO$_2$	6.942E−02	6.872E−02	6.793E−02	9.575E−02	− 1.01
EI	CO	145.287	139.790	5.125	6.887	− 3.78
EI	Ozone	278.890	288.802	5.083	6.255	3.55
EI	NO$_2$	6.271E+15	5.085E+15	1.108E+15	9.243E+14	− 18.91
EI	SO$_2$	1.264E−01	9.122E−02	1.173E−01	1.278E−01	− 27.85
NEI	CO	151.972	149.536	4.531	5.948	− 1.60
NEI	Ozone	281.303	294.312	4.240	5.826	4.62
NEI	NO$_2$	4.435E+15	4.268E+15	6.525E+14	8.022E+14	− 3.76
NEI*	SO$_2$	− 1.673E−03	− 4.669E−03	6.075E−02	1.054E−01	–

*Due to interference of two absorption signal when matching measured spectrum with absorption cross sections of SO$_2$ and ozone and low concentration of SO$_2$ results negative SO$_2$ slant column values, with an error of the same magnitude. Hence for such cases results has been omitted

activities and heavy vehicular movements lead to higher concentrations of NO$_2$ and CO in the IGP region [43]. Due to this, a strong positive correlation has been observed in the region. A positive average correlation coefficient of 0.54 has also been observed over the NEI. It may be due to a higher concentration of CO which is transported by wind from neighboring regions. NI shows a positive correlation between ozone and CO during the lockdown period. Ozone in the Tropospheric mostly depends on the concentration of NO$_2$.

4 Conclusions

The aerosol and air Pollution analysis conducted in the present study over pan India indicates that air quality was improved during the lockdown imposed due the COVID-19 pandemic. Overall, the COVID-19 lockdown had reduced human activity due to which, lower air pollutants concentration has been observed over pan India, especially in NI. At the early stage of the lockdown period, the

Central Pollution Control Board (CPCB) of India has also reported that, after a long time, major cities in the country have shown good air quality index. From the study, it can be concluded that;

1. Aerosol loading in the atmosphere as those represented by AOD and AI retrieval from MODIS Terra and OMI show relatively lower values during the lockdown period compared to its value in the same period in previous years. Thus, lower values of AOD and AI during the lockdown period indicate that anthropogenic activity is mainly responsible for aerosol loading over pan India. Hence, this study corroborates this hypothesis through spatial analysis of satellite derived data.

2. Even North India's most polluted region IGP also displays remarkably lower AI during the lockdown period. The lower value of AI in India is mainly due to the lockdown and partially due to rainfall events during the lockdown over some parts of India primarily over NI, EI and SI. It can also be concluded that due to lockdown during COVID-19, AOD has decreased by approximately
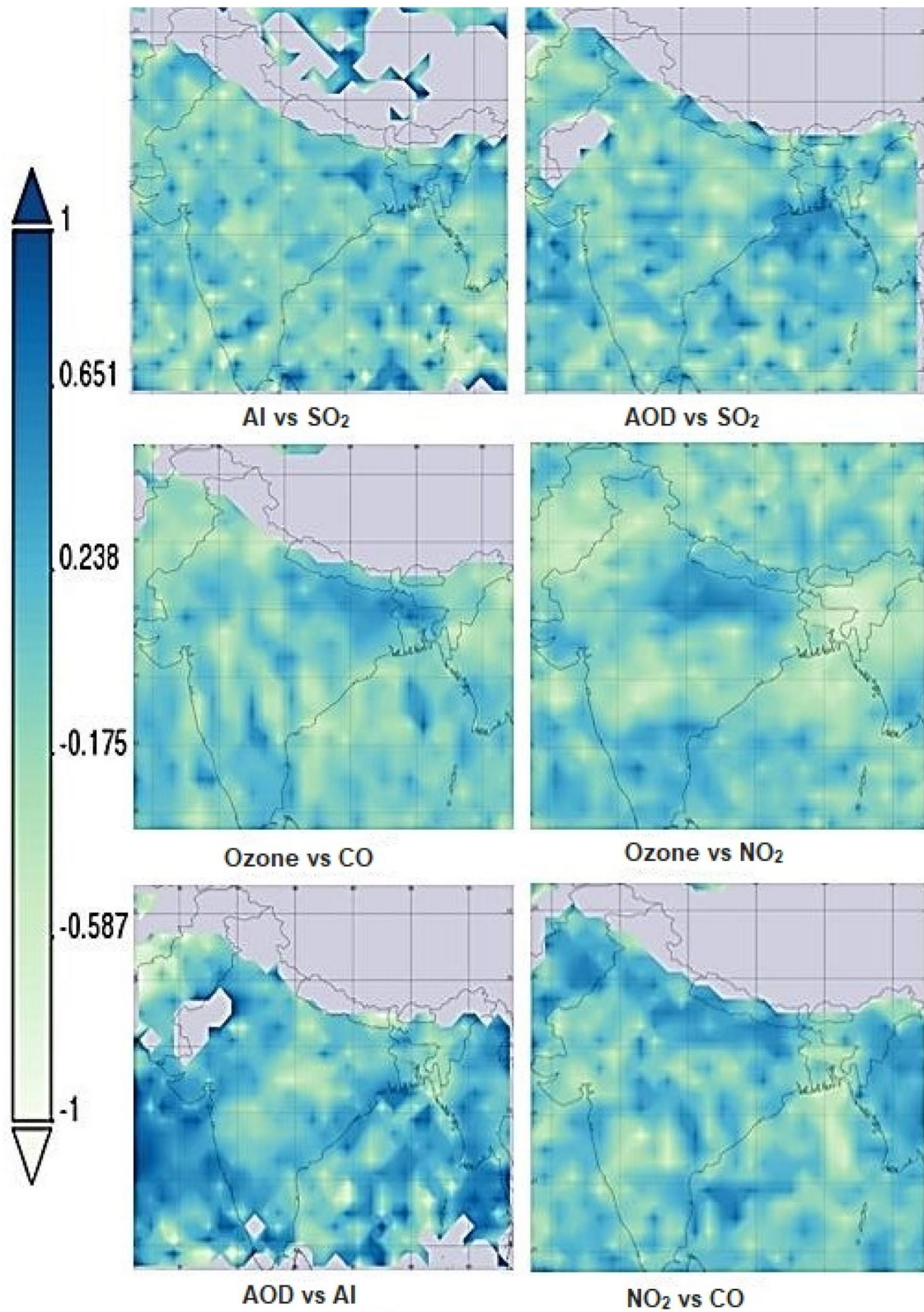
Fig. 9 Spatial correlation of aerosol variable and gaseous pollutant during lockdown period (23 March to 3 May 2020)

26.65% over NI followed by 18% (WI) and 17% (SI) and less reduction is observed over CI (7 %).

3. The present study also shows that aerosol parameters such as AOD, AI and air pollutants CO, SO_2 and NO_2 recorded lower values during the lockdown except ozone which shows increasing value primarily over NI and NEI. Higher reduction in NO_2 has been observed over NI (20.17%), CI (16.26%) and EI (18.91%) whereas reduction in SO_2 over CI (31%), WI (47%) and EI (27%). From the spatial correlation map, it can be concluded that there is a considerable variation in the values of all air pollutants during the lockdown period when compared to these values in period 2016–2019 mainly over the NI where more human activities are observed. The present study related to aerosol concentration estimation during lockdown period of COVID-19 concludes that anthropogenic activities are primarily responsible for the deterioration of air quality over different parts of India. Therefore, control measures can lead to a better climate and environment.

Declarations

Conflict of interest The authors declare that they have no conflict of interests.

References

1. Zhang, J. P., Zhu, T., Zhang, Q. H., Li, C. C., Shu, H. L., Ying, Y., et al. (2012). The impact of circulation patterns on regional transport pathways and air quality over Beijing and its surroundings. *Atmospheric Chemistry and Physics, 12*(11), 5031–5053.
2. WHO (2016). WHO global urban ambient air pollution database (update 2016). http://www.who.int/phe/health_topics/outdoorair/databases/cities/en/.
3. Guttikunda, S. K., Nishadh, K. A., & Jawahar, P. (2019). Air pollution knowledge assessments (APnA) for 20 Indian cities. *Urban Climate, 27*, 124–141. https://doi.org/10.1016/j.uclim.2018.11.005
4. Kumar, R. P., Perumpully, S. J., Samuel, C., & Gautam, S. (2023). Exposure and health: A progress update by evaluation and scientometric analysis. *Stochastic Environmental Research and Risk Assessment, 37*(2), 453–465.
5. Yuda, M. (2019). Asian countries rush to fight toxic air pollution. Accessed from https://asia.nikkei.com/Economy/Asian-countries-rush-to-fight-toxic-air-pollution.
6. Ukaogo, P. O., Ewuzie, U., & Onwuka, C. V. (2020). Environmental pollution: Causes, effects, and the remedies. In: *Microorganisms for sustainable environment and health* (pp. 419–429). Elsevier. https://doi.org/10.1016/B978-0-12-819001-2.00021-8.
7. Patel, V. K., Taksal, P. A., Londhe, D. S., & Katpatal, Y. B. (2021). Spatio-temporal variation of aerosols in ENSO events over Western India using satellite data. *Journal of Environmental Engineering and Science, 16*(2), 77–84.
8. Pope, C. A., Ezzati, M., & Dockery, D. W. (2009). Fine particulate air pollution and life expectancy in the United States, New England. *Journal of Medicine, 360*, 376–386. https://doi.org/10.1056/NEJMsa0805646
9. Robert, D. B., Sanjay, R., Pope, C. A., Jeffrey, R. B., Aruni, B., Ana, V. D., et al. (2010). Particulate matter air pollution and cardiovascular disease: An update to the scientific statement from the American Heart Association. *Circulation, 121*, 2331–2378. https://doi.org/10.1161/CIR.0b013e3181dbece1
10. Singh, R., Singh, V., Gautam, A. S., Gautam, S., Sharma, M., & Soni, P. S., et al. (2022). Temporal and spatial variations of satellite-based aerosol optical depths, angstrom exponent, single scattering albedo, and ultraviolet-aerosol index over five polluted and less-polluted cities of Northern India: Impact of urbanization and climate change. *Aerosol Science and Engineering,* pp. 1–19.
11. Seinfeld, J. H., & Pandis, S. N. (2016). *Atmospheric chemistry and physics: From air pollution to climate change*. Wiley.
12. Kaufman, Y. J., Tanre, D., & Boucher, O. (2002). A satellite view of aerosols in the climate system. *Nature, 419*, 215–223. https://doi.org/10.1038/nature01091
13. Charlson, R. J., et al. (1992). Climate forcing by anthropogenic aerosols. *Science, 255*, 423–430. https://doi.org/10.1126/science.255.5043.423
14. Hansen, J. E., Sato, M., Lacis, A., Ruedy, R., Tegen, I., & Matthews, E. (1998). Climate forcings in the industrial era. *Proceedings of the National Academy of Sciences of the United States of America, 95*(22), 12753–12758.
15. Kaufman, Y. J., et al. (2003). Fire and smoke observed from the Earth Observing System MODIS instrument: Products, validation, and operational use. *International Journal of Remote Sensing, 2*(8), 1765–1781. https://doi.org/10.1080/01431160210144741
16. Jones, A., & Slingo, A. (1996). Predicting cloud-droplet effective radius and indirect sulphate aerosol forcing using a general circulation model. *Quarterly Journal of the Royal Meteorological Society, 122*, 1573–1595. https://doi.org/10.1002/qj.49712253506
17. Gupta, P., Christopher, S. A., Wang, J., Gehrig, R., Lee, Y. C., & Kumar, N. (2006). Satellite remote sensing of particulate matter and air quality over global cities. *Atmospheric Environment, 40*(30), 5880–5892. https://doi.org/10.1016/j.atmosenv.2006.03.016
18. Ahmad, S. P., Torres, O., Bhartia, P. K., Leptoukh, G., & Kempler, S. J. (2006). Aerosol index from TOMS and OMI measurements. In *Proceedings of the 86th AMS annual meeting,* February 2006.
19. Torres, O., Bhartia, P. K., Herman, J. R., Sinyuk, A., Ginoux, P., & Holben, B. (2002). A long–term record of aerosol optical depth from TOMS observations and comparison to AERONET measurements. *Journal of the Atmospheric Sciences, 59*, 398–413. https://doi.org/10.1175/1520-0469(2002)059%3c0398:ALTROA%3e2.0.CO;2
20. Torres, O., Bhartia, P. K., Herman, J. R., Ahmad, Z., & Gleason, J. (1998). Derivation of aerosol properties from satellite measurements of backscattered ultraviolet radiation: Theoretical basis. *Journal of Geophysical Research-Atmospheres, 103*, 17099–17110. https://doi.org/10.1029/98JD00900
21. Baddock, M. C., Bullard, J. E., & Bryant, R. G. (2009). Dust source identification using MODIS: A comparison of techniques applied to the Lake Eyre Basin, Australia. *Remote Sensing of Environment, 113*, 1511–1528. https://doi.org/10.1016/j.rse.2009.03.002
22. Hsu, N. C., Herman, J. R., Torres, O., Holben, B. N., Tanre, D., Eck, T. F., Smirnov, A., Chatenet, B., & Lavenu, F. (1999). Comparisons of the TOMS aerosol index with Sun–photometer aerosol optical thickness: Results and applications. *Journal of Geophysical Research-Atmospheres, 104*(D6), 6269–6279. https://doi.org/10.1029/1998JD200086
23. Washington, R., Todd, M., Middleton, N. J., & Goudie, A. S. (2003). Dust–storm source areas determined by the total ozone monitoring spectrometer and surface observations. *Annals of the

Association of American Geographers, 93, 297–313. https://doi.org/10.1111/1467-8306.9302003

24. Sarath, K. G., & Ramani, V. K. (2014). Source emissions and health impacts of urban air pollution in Hyderabad, India. *Air Quality Atmosphere and Health, 7*(2), 195–207. https://doi.org/10.1007/s11869-013-0221-z

25. Gautam, S., Patra, A. K., & Kumar, P. (2018). Status and chemical characteristics of ambient PM2.5 pollutions in China: A review. *Environment, Development and Sustainability.* https://doi.org/10.1007/s10668-018-0123-1

26. Gautam, S. (2020). The influence of COVID-19 on air quality in India: A boon or inutile. *Bulletin of Environmental Contamination and Toxicology, 104*, 724–726. https://doi.org/10.1007/s00128-020-02877-y

27. Chelani, A. B., & Gautam, S. (2022). The influence of meteorological variables and lockdowns on COVID-19 cases in urban agglomerations of Indian cities. *Stochastic Environmental Research and risk Assessment, 36*(9), 2949–2960.

28. Jethva, H., Chand, D., Torres, O., Gupta, P., Lyapustin, A., & Patadia, F. (2018). Agricultural burning and air quality over northern India: A synergistic analysis using NASA's a-train satellite data and ground measurements. *Aerosol and Air Quality Research, 18*, 1756–1773. https://doi.org/10.4209/aaqr.2017.12.0583

29. Sayer, A. M., Thomas, G. E., Palmer, P. I., & Grainger, R. G. (2010). Some implications of sampling choices on comparisons between satellite and model aerosol optical depth field. *Atmospheric Chemistry and Physics, 10*, 10705–10716. https://doi.org/10.5194/acp-10-10705-2010

30. Herman, J. R., & Celarier, E. A. (1997). Earth surface reflectivity climatology at 340–380 nm from TOMS data. *Journal of Geophysical Research-Atmospheres, 102*, 28003–28011. https://doi.org/10.1029/97JD02074

31. de Graaf, M., Stammes, P., Torres, O., & Koelemeijer, R. B. A. (2005). Absorbing Aerosol Index: Sensitivity analysis, application to GOME and comparison with TOMS. *Journal of Geophysical Research-Atmospheres.* https://doi.org/10.1029/2004JD005178

32. Levelt, P. F., Hilsenrath, E., Leppelmeier, G. W., Van Den Oord, G. H. J., Bhartia, P. K., Tamminen, J., De Haan, J. F., & Veefkind, J. P. (2006). Science objectives of the ozone monitoring instrument. *IEEE Transactions on Geoscience and Remote Sensing, 44*(1199–1208), 2006a. https://doi.org/10.1109/TGRS.2006.872336

33. Levelt, P. F., Van Den Oord, G. H. J., Dobber, M. R., Mälkki, A., Visser, H., Vries, J. D., Stammes, P., Lundell, J. O. V., & Saari, H. (2006). The ozone monitoring instrument. *IEEE Transactions on Geoscience and Remote Sensing, 44*(1093–1101), 2006b. https://doi.org/10.1109/TGRS.2006.872333

34. Veefkind, P. (2006). OMI/Aura Ozone (O3) DOAS Total Column 1-Orbit L2 Swath 13×24 km V003, Greenbelt, MD, USA. Goddard Earth Sciences Data and Information Services Center (GES DISC). https://doi.org/10.5067/Aura/OMI/DATA2012

35. Krotkov, N. A., Cam, S. A., Krueger, A. J., Bhartia, P. K., & Yang, K. (2006). Band residual difference algorithm for retrieval of SO_2 from the Aura Ozone Monitoring Instrument (OMI). *IEEE Transactions on Geoscience and Remote Sensing, 44*, 1259–1266. https://doi.org/10.1109/TGRS.2005.861932

36. Intergovernmental Panel on Climate Change (2001). Climate Change 2001: The Scientific Basis: Contribution of Working Group I to the Third Assessment Report of the Intergovernmental Panel on Climate Change, edited by J. T. Houghton et al., Cambridge Univ. Press, New York.

37. Thomas, A., Sarangi, C., & Kanawade, V. P. (2019). Recent increase in winter hazy days over Central India and the Arabian Sea. *Scientific Reports, 9*(1), 1–10.

38. The AERONET Aerosol Optical Depth data https://aeronet.gsfc.nasa.gov

39. Choudhary, A., Kumar, P., Sahu, S. K., Pradhan, C., Joshi, P. K., Singh, S. K., et al. (2022). Health risk appraisal associated with air quality over coal-fired thermal power plants and coalmine complex belts of urban-rural agglomeration in the eastern coastal state of Odisha. *India. Atmosphere, 13*(12), 2064.

40. Crutzen, P. J. (1979). The role of NO and NO_2 in the chemistry of the troposphere and stratosphere. *Annual review of earth and planetary sciences, 7*, 443–472.

41. Arunkumar, M., & Dhanakumar, S. (2021). Influence of meteorology, mobility, air mass transport and biomass burning on PM2.5 of three north Indian cities: Phase-wise analysis of the COVID-19 lockdown. *Environmental Monitoring and Assessment, 193*(9), 618.

42. Zhao, D., Schmitt, S. H., Wang, M., Acir, I. H., Tillmann, R., Tan, Z., et al. (2018). Effects of NOx and SO_2 on the secondary organic aerosol formation from photooxidation of α-pinene and limonene. *Atmospheric Chemistry and Physics, 18*(3), 1611–1628. https://doi.org/10.5194/acp-18-1611-2018

43. Mor, S., Singh, T., Bishnoi, N. R., Bhukal, S., & Ravindra, K. (2022). Understanding seasonal variation in ambient air quality and its relationship with crop residue burning activities in an agrarian state of India. *Environmental Science and Pollution Research, 29*, 4145–4158.